# Microcystic Cyanobacteria Extract Induces Cytoskeletal Disruption and Intracellular Glutathione Alteration in Hepatocytes

***Wen-Xing Ding, Han-Ming Shen, and Choon-Nam Ong***

Center for Environmental and Occupational Health, Department of Community, Occupational and Family Medicine, National University of Singapore, Singapore

**Microcystins are a group of highly liver-specific toxins, although their exact mechanisms of action remain unclear. We examined the effects of microcystic cyanobacteria extract (MCE) collected from a contaminated water source on the organization of cellular microtubules (MTs) and microfilaments (MFs) in hepatocytes. We also investigated the effects on lactate dehydrogenase (LDH) leakage and intracellular glutathione (GSH). Primary cultured rat hepatocytes exposed to MCE (equivalent to 125 μg/mL lyophilized algae cells) showed a characteristic disruption of MTs and MFs in a time-dependent manner. Under these conditions, MCE caused aggregation of MTs and MFs and a severe loss of MTs in some cells. Moreover, MCE-induced cytoskeletal alterations preceded the LDH leakage. On the other hand, the treatment of cells with MCE led to a dose-dependent increase of intracellular GSH. However, time-course study showed a biphasic change of intracellular GSH levels with a significant increase in the initial stage followed by a decrease after prolonged treatment. Furthermore, pretreatment with *N*-acetylcystein (NAC), a GSH precursor, significantly enhanced the intracellular GSH level and decreased the MCE-induced cytotoxicity as well as cytoskeleton changes. In contrast, buthionine-(*S,R*)-sulfoximine, a specific GSH synthesis inhibitor, increased the cell susceptibility to MCE-induced cytotoxicity by depleting the intracellular GSH level. These findings suggest that intracellular GSH plays an important role in MCE-induced cytotoxicity and cytoskeleton changes in primary cultured rat hepatocytes. Increasing intracellular GSH levels protect cells from MCE-induced cytotoxicity and cytoskeleton changes.**
***Key words*: cyanobacteria, cytoskeleton, glutathione, hepatocytes, hepatotoxicity, microcystin.**
***Environ Health Perspect* 108:605–609 (2000). [Online 25 May 2000]**
***http://ehpnet1.niehs.nih.gov/docs/2000/108p605-609ding/abstract.html***

The occurrence of heavy freshwater blooms of cyanobacteria (blue-green algae) has been well reported in many parts of the world (*1*). Among the toxic blue-green algae, *Microcystis* is the most common genera producing microcystins, a group of toxins with strong hepatotoxicity (*1,2*). These toxins are able to cause the death of domestic and wild animals as well as human illness (*3*). Recently, it has been reported that dialysis patients in Brazil died of acute hepatic failure due to cyanobacteria contamination of the water used for dialysis (*4,5*). Recent epidemiologic studies have suggested that the cyanobacteria-contaminated water could be related to the high incidence of primary liver cancer in certain areas of China (*6,7*). Our previous study also showed that microcystic cyanobacteria extract (MCE) of a water source in China had potent genotoxicity (*8*).

Microcystins are highly liver specific and their hepatotoxicity has been well studied (*9–11*). However, the exact mechanisms by which microcystins cause hepatotoxicity have not been fully elucidated. One of the extensively studied mechanisms is that microcystins are potent inhibitors of protein phosphatase 1 and 2A, which lead to the increase of protein phosphorylation (*1*). The hyperphosphorylation of proteins have been attributed to the destruction of intermediate filaments (IFs) (*12,13*). Microcystin-disrupted microfilaments (MFs) have also been reported (*14,15*). In contrast, only one study showed that microtubules (MTs) were disrupted by microcystin-LR in primary cultured rat hepatocytes and several nonhepatocyte cell lines (*16*). However, at present, there are no studies to show that MF and MT proteins have also been phosphorylated by microcystin. Therefore, it is possible that there is another mechanism, besides protein phosphorylation, which contributes to microcystin-disrupted MFs and MTs.

The cytoskeleton consists of three major structural elements: MTs, MFs, and IFs. These elements play an important role in maintaining cellular architecture and internal organization, cell shape, motility, cell division, and many other processes (*17*). There are many cysteine residues in the cytoskeleton proteins, and certain tubulin–SH groups are crucial for its polymerization *in vitro* (*18*). Cellular-reduced glutathione (GSH) is important for the regulation of cytoskeleton organization (*19*). Perturbing the cellular redox status by depleting intracellular GSH provoked disruption of MFs in human fibroblasts (*20*). It has been reported that certain metal carcinogens such as cadmium and arsenite disrupted cytoskeletal structures, and those changes had a close relationship with the cellular GSH level alterations (*21,22*).

At present, there are several lines of evidence suggesting that GSH may play a critical role in the detoxification of microcystins. Microcystins could conjugate with GSH in cell-free systems or in the liver tissue *in vivo* (*23–25*), which substantially reduced its cytotoxicity (*23*). Moreover, our previous studies showed that MCE induced lipid peroxidation and reactive oxygen species (ROS) formation in primary cultured rat hepatocytes (*26,27*), suggesting the possible effect of MCE on cellular redox status. However, so far there is no systematic study on the role of GSH in the hepatotoxicity of microcystins and its association with the cytoskeleton.

Thus, in the present study, we aimed to determine the involvement of GSH on the MCE-induced cytotoxicity and disruption of MTs and MFs in primary cultured hepatocytes. In our study, the intracellular GSH level in rat hepatocytes was modulated by *N*-acetylcystein (NAC), a GSH precursor, and buthionine-(*S,R*)-sulfoximine (BSO), a specific GSH synthesis inhibitor. Data from these experiments provide direct evidence showing that GSH is closely involved in MCE-induced cytoskeletal disruption and hepatotoxicity.

## Materials and Methods

***Chemicals.*** We purchased William's medium E, insulin, collagenase, Hepes, L-glutamine, penicillin, and streptomycin, NAC, BSO, GSH, *o*-phthalaldehyde (OPT), and mouse fluorescein isothiocyanate (FITC) conjugate monoclonal anti-β-tubulin from Sigma (St. Louis, MO). We purchased fetal bovine serum (FBS) from Gibco BRL (Life Technologies, Gaithersburg, MD) and Alex 488 phalloidin and propidium iodide (PI) from Molecular Probes (Eugene, OR). All other common chemicals were reactive agent grade and were purchased from Merck (Darmstadt, Germany).

Address correspondence to C.N. Ong, Center for Environmental and Occupational Health, Department of Community, Occupational and Family Medicine, MD3, National University of Singapore, Singapore 117597, Singapore. Telephone: 65 8744982. Fax: 65 7791489. E-mail: cofongcn@nus.edu.sg

We thank E. Cornie and X. Wen for technical assistance in the confocal microscopy.

W-X. Ding is supported by a research scholarship from National University of Singapore.

Received 23 December 1999; accepted 1 February 2000.

***Sampling of cyanobacteria.*** In early fall 1995 we collected the blue-green algae from Dianshan Lake, one of the main water supply sources for Shanghai, during a water bloom period. Shanghai is the largest city in the People's Republic of China. The water blooms were dominated by *Microcystis aeruginosa* (determined by microscopic examination) and the algae cells were lyophilized for toxins extraction.

***Extraction of toxins.*** We extracted the toxins as described by Ding et al. (*8*). Briefly, we suspended lyophilized algae cells (25 mg) in 2.5 mL *n*-butanol:methanol:water (1:4:15, v/v/v), then the suspension was centrifuged at 16,000*g* for 30 min. The supernatant from three extractions was pooled together and then passed through a preconditioned Sep-Pak C18 cartridge (3 mL tube; Supelco, Bellefonte, PA) to eliminate some impurities by washing with 3 mL 20% methanol, then eluted with 10 mL pure methanol. Finally, the methanol elute was evaporated to dryness at 56°C and dissolved in 2 mL distilled and deionized water.

***Liver perfusion and primary rat hepatocyte culture.*** Liver perfusion and primary rat hepatocyte culture were carried out as reported earlier (*27*). The cells were plated at a density of $4 \times 10^6$ cells/75 $cm^2$ flask (Corning, Stony Brook, NY). After preincubation for 2 hr in 10 mL complete Williams' medium E (supplemented with 2 mM L-glutamine, 0.02 IU insulin/mL, and 10% FBS), we washed the flasks with prewarmed Hepes buffer (pH 7.4) to remove the unattached dead cells. The hepatocytes were then incubated in serum-free Williams' medium E with various treatments.

***Treatments.*** For the dose–response study, we incubated cells with three doses of MCE for 6 hr: the low concentration (equivalent to 1.25 µg lyophilized algae cells/mL), the moderate concentration (equivalent to 12.5 µg lyophilized algae cells/mL), and the high concentration (equivalent to 125 µg lyophilized algae cells/mL). For the time-course study, we exposed hepatocytes to high concentration of MCE (125 µg lyophilized algae cells/mL) for designated periods of time.

To study the role of GSH in modulating MCE-induced cytotoxicity, we pretreated cells with NAC 10 mM or BSO 2.5 mM for 6 hr, then washed them with Hepes buffer once. The cells were further exposed to the high concentration of MCE (125 µg/mL) for another 6 hr. We examined the cytotoxicity and intracellular GSH levels.

***Detection of cytoskeleton disruption.*** Primary hepatocytes on cover slides (12 × 12 mm) in 35-mm Petri dishes were preincubated for 2 hr in 5 mL Williams' medium E supplemented with 10% FBS, then washed with Hepes buffer once. We then incubated the hepatocytes in serum-free Williams' medium E with the high concentration of MCE for up to 6 hr. Both control and treated cells were processed for fluorescent staining for MT and MF visualization. To study the effects of NAC on MCE-induced MT and MF changes, we pretreated the cells with 10 mM NAC for 6 hr and washed them once with Hepes buffer. The cells were then exposed to MCE for another 6 hr.

MFs were determined according to the protocol provided by the manufacturer (Molecular Probes) with certain modifications. Briefly, cells on cover slides were washed twice with phosphate-buffered saline (PBS) and then fixed with freshly prepared 3.7% paraformaldehyde in PBS for 30 min. The cells were permeabilized with 0.1% Triton × 100 in PBS for 15 min and then blocked with 1% bovine serum albumin in PBS for 30 min at room temperature. The MFs and nuclei on cover slides were then stained with Alex 488 Phalloidin (1:40 dilution) and 10 µg/mL PI, respectively.

We labeled MTs according to Li and Chou (*21*), with modifications. Briefly, the cells were first washed with PBS and with a microtubule stabilizing buffer (PM2G) containing 0.1 M Pipes, 1 mM $MgSO_4$, 2 M glycerol, and 2 mM EGTA (pH 6.9). The cells were fixed with freshly prepared 3.7% paraformaldehyde in PM2G for 30 min and washed with PBS once. The cells were then permeabilized with 0.5% NP-40 in PBS. MTs were labeled with mouse FITC conjugate monoclonal anti-β-tubulin (1:25 dilution) for 1 hr at room temperature.

For both MF and MT staining, we mounted the coverslides on glass slides with a drop of mounting solution (PBS:glycerol, 3:1). We then examined the cytoskeletal morphologies with an Olympus confocal microscope (Olympus, Tokyo, Japan) equipped with a krypton/argon laser and an Olympus 60 × numerical aperture, 1.25 Planapo objective. Excitation intensity was set to provide bright pixels without saturation.

***Determination of cytotoxicity.*** We determined the cytotoxicity of MCE on cultured rat hepatocytes by the percentage of lactate dehydrogenase (LDH) leakage from cells into the medium (*27*), which was calculated according to the following formula: %LDH leakage = (LDH activity present in the medium after treatment/total LDH activity at the same time) × 100.

***Determination of intracellular GSH content.*** We determined the intracellular GSH content according to the method of Hissin and Hilf (*28*). The stock solution of the fluorescent probe OPT was freshly prepared in methanol (1 mg/mL). After various designated treatment, cells were collected using cell scrapers and washed twice with cold PBS and then suspended in 0.1 M sodium phosphate/5 mM EDTA (pH 8.0). After ultrasonication, we mixed 0.75 mL cell homogenate with 0.2 mL 25% metaphosphoric acid to precipitate the proteins. We monitored the fluorescence intensity of OPT with excitation wavelength at 350 nm and emission wavelength at 420 nm. We established a GSH calibration curve using standard GSH, and the GSH concentration was expressed as nanomole per $10^6$ cells.

***Statistical analysis.*** We repeated each experiment at least 3 times and the numerical data were presented as means ± SD and analyzed using Student's *t*-test. We considered a $p$-value < 0.05 statistically significant.

## Results

***MCE-induced dose- and time-dependent increase of LDH leakage.*** When we treated cells with MCE for 6 hr, there was no significant change of LDH leakage in the low (1.25 µg lyophilized cells/mL) and the moderate concentration of MCE (12.5 µg lyophilized cells/mL) (Figure 1A). For cells treated with the high concentration of MCE (125 µg lyophilized cells/mL), there was a significant increase of LDH leakage ($p < 0.05$). Figure 1B shows a time-dependent increase of LDH leakage when rat hepatocytes were treated with 125 µg MCE for 24 hr. The LDH leakage was approximately 70% and the control group remained a constant low LDH leakage level (around 10%) at 24 hr. In our experiments, the total LDH activity is mainly dependent on the cell number added into each flask at the beginning of the treatment. The total LDH remained relatively stable under our experimental conditions in the relatively short culture time of our experiments.

***MCE-induced dose- and time-dependent alterations of intracellular GSH.*** A dose-dependent increase of intracellular GSH in MCE-treated hepatocytes is shown in Figure 2A. Figure 2A clearly shows that MCE increased the intracellular GSH level markedly after a 6-hr treatment with 12.5 and 125 µg MCE ($p < 0.05$). In contrast, time-course studies showed that cells exposed to the high concentration of MCE (125 µg lyophilized cells/mL) exhibited a biphasic response in their intracellular GSH. The intracellular GSH showed no significant change until 3 hr, when it started to increase sharply and reached the maximum level at 6 hr. After 12-hr treatment, the intracellular GSH level started to decrease but was still significantly higher than the control ($p < 0.05$). After 24-hr treatment, the intracellular GSH level reduced drastically (Figure 2B). Similar patterns of intracellular GSH level changes were also observed when GSH was measured using monochlorobine in flow cytometry (results not shown).

***Alterations in cytoskeletal organization.*** Figure 3 shows the morphologies of cells stained for MTs and MFs and nuclei. The normal hepatocytes contain a highly organized network of MTs that are distributed evenly in a wavy and curving pattern (Figure 3A). In hepatocytes treated with 125 µg MCE, the filamentous pattern of MTs was disrupted and collapsed toward the interior of the cells after 1 hr treatment (Figure 3C). When treated with 125 µg MCE for 3 hr, we observed a noticeable reduction in the number of MTs in the cells, whereas densely aggregated MTs appeared to retract around the nucleus. Moreover, in some cells all MTs were lost and only the nuclei were stained (Figure 3E, arrow). This effect was more evident when cells were treated for 6 hr (Figure 3G). In contrast, when cells were pretreated with NAC for 6 hr, the lost and aggregated MTs caused by MCE were significantly protected (Figure 3I).

Figure 3B shows the normal MF organization in untreated cells. MFs in the untreated cells show uniform distribution and good organization. Exposure of cells to MCE (125 µg/mL) for 1 hr produced severe MF disorganization, characterized by the concentration of actin fibers inside the plasma membrane of some cells and the aggregation or collapse into the interior of the cells (Figure 3D). These rosettelike aggregates of actin fibers in some cells emerged from the cytoplasm and protruded into the blebs when the cells were treated with MCE for 3 hr (Figure 3F). After 6 hr treatment with MCE, we observed an obvious reduction of MFs (Figure 3H). However, much better organized MFs reappeared when the cells were pretreated with NAC for 6 hr (Figure 3J). We found similar morphologic changes of MTs and MFs when the hepatocytes were treated with pure microcystin-LR at 0.1 µM (data not shown)

***Effects of NAC and BSO on MCE-induced cytotoxicity.*** To assess the role of GSH in modulating MCE-induced cytotoxicity, we pretreated cultured rat hepatocytes with NAC (10 mM) or BSO (2.5 mM) for 6 hr and washed them once with Hepes buffer. The cells were then further exposed to 125 µg MCE for another 6 hr. Figure 4A shows the effects of NAC and BSO on MCE-induced cytotoxicity, as measured by the percentage of LDH leakage. NAC or BSO alone did not significantly cause the LDH leakage in rat hepatocytes. However, when cells were pretreated with NAC for 6 hr, the cytotoxicity induced by MCE was significantly reduced ($p < 0.05$). In contrast, when cells were pretreated with BSO, the LDH leakage was enhanced significantly as compared to cells treated with MCE only ($p < 0.05$). The results indicate that intracellular GSH protects the cells against MCE-induced cytotoxic effects, and depleting intracellular GSH leads to increased susceptibility to cell damage.

We also investigated the effect of NAC and BSO pretreatment on MCE-induced intracellular GSH changes. Figure 4B shows that NAC enhanced the intracellular GSH level, whereas BSO decreased the intracellular GSH level. Furthermore, when cells were pretreated with NAC and MCE, there was a significant increase of intracellular GSH ($p < 0.05$). In contrast, we observed that the intracellular GSH level decreased significantly when cells were exposed to BSO and MCE ($p < 0.05$).

## Discussion

In this study we have shown that hepatocytes exposed to MCE exhibit characteristic alterations in cytoskeletal morphology caused by the disappearance of regular filamentous structure soon after MCE treatment. We observed severe reorganization of MTs and aggregation of MFs after prolonged treatment. These results are in agreement with previous reports using pure microcystin-LR (*14,16*), and are in line with our earlier finding using MCE (*26,27*), where microsystin-LR was identified as the main component (*8*).

Microcystin-LR is a strong inhibitor of protein phosphatase 1 and 2A and eventually causes hyperphosphorylation of cytosolic and cytoskeletal proteins (*14*). Phosphorylation is an important mechanism regulating the organization of cytoskeleton. The IFs proteins can be phosphorylated and the phosphorylation status is closely correlated with its disassembly (*29*). Toivola et al. recently reported that microcystin-LR induced hyperphosphorylation of keratin 8 and 18, which eventually led to the disruption of IFs. In addition, phosphorylation of microtubule-associated proteins (MAPS) and actin-associated proteins may induce alterations of polymerization of MTs and distribution of MFs (*30,31*). However, it is still unclear at this stage whether the observed MT and MF changes induced by microcystin are a result of increased phosphorylation of MAPS with the subsequent destabilization of MTs and MFs. An earlier study showed that phosphorylation of tubulin and MAPS was not changed by calyculin A, another potent inhibitor of protein phosphatase 1 and 2A (*12*), although the concentration used (50 nM) was relatively low. On the other hand, several studies suggested that oxidative stress could affect actin dynamics by markedly inhibiting the assembly of actin monomers and eventually disrupted its

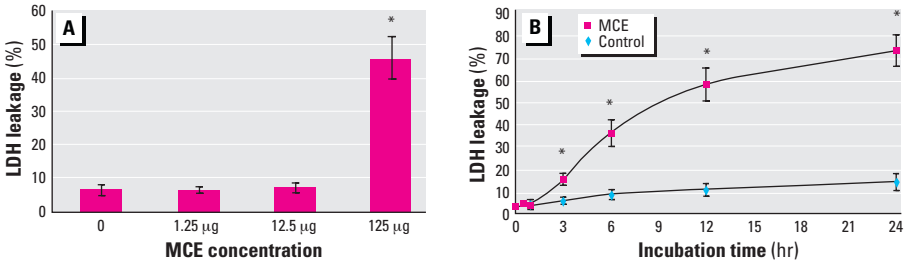


**Figure 1.** Dose–response and time-course alterations of LDH leakage in MCE-treated cultured rat hepatocytes. (*A*) Dose response of LDH leakage: the cells were exposed to three different concentrations of MCE for 6 hr, and data are means ± SD ($n = 6$). (*B*) The time course of LDH leakage: the cells were treated with MCE (equivalent to 125 µg/mL) up to 24 hr. Data are means ± SD of three independent experiments ($n = 3$) (Student's *t*-test).

*$p < 0.05$ as compared to the control group (one-way analysis of variance with Scheffe's test).

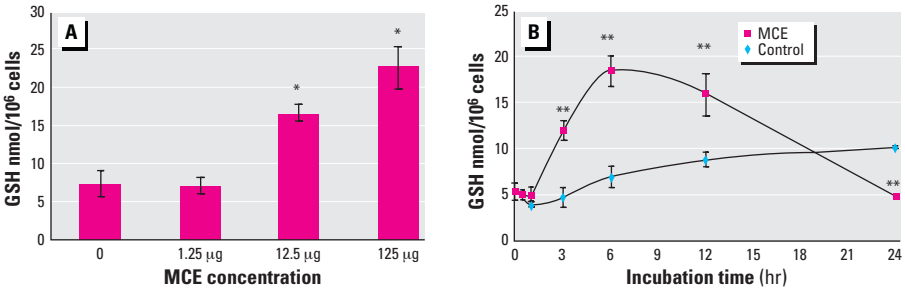


**Figure 2.** Dose response and time course of intracellular GSH alterations induced by MCE. (*A*) Dose response of GSH alterations: the cells were exposed to three different concentrations of MCE for 6 hr, and data are means ± SD ($n = 6$). (*B*) The time course of intracellular GSH alterations; data are means ± SD of three independent experiments ($n = 3$).

*$p < 0.05$ as compared to the control group (one-way analysis of variance with Scheffe's test). **$p < 0.05$ as compared to the control group at each time point (Student's *t*-test).

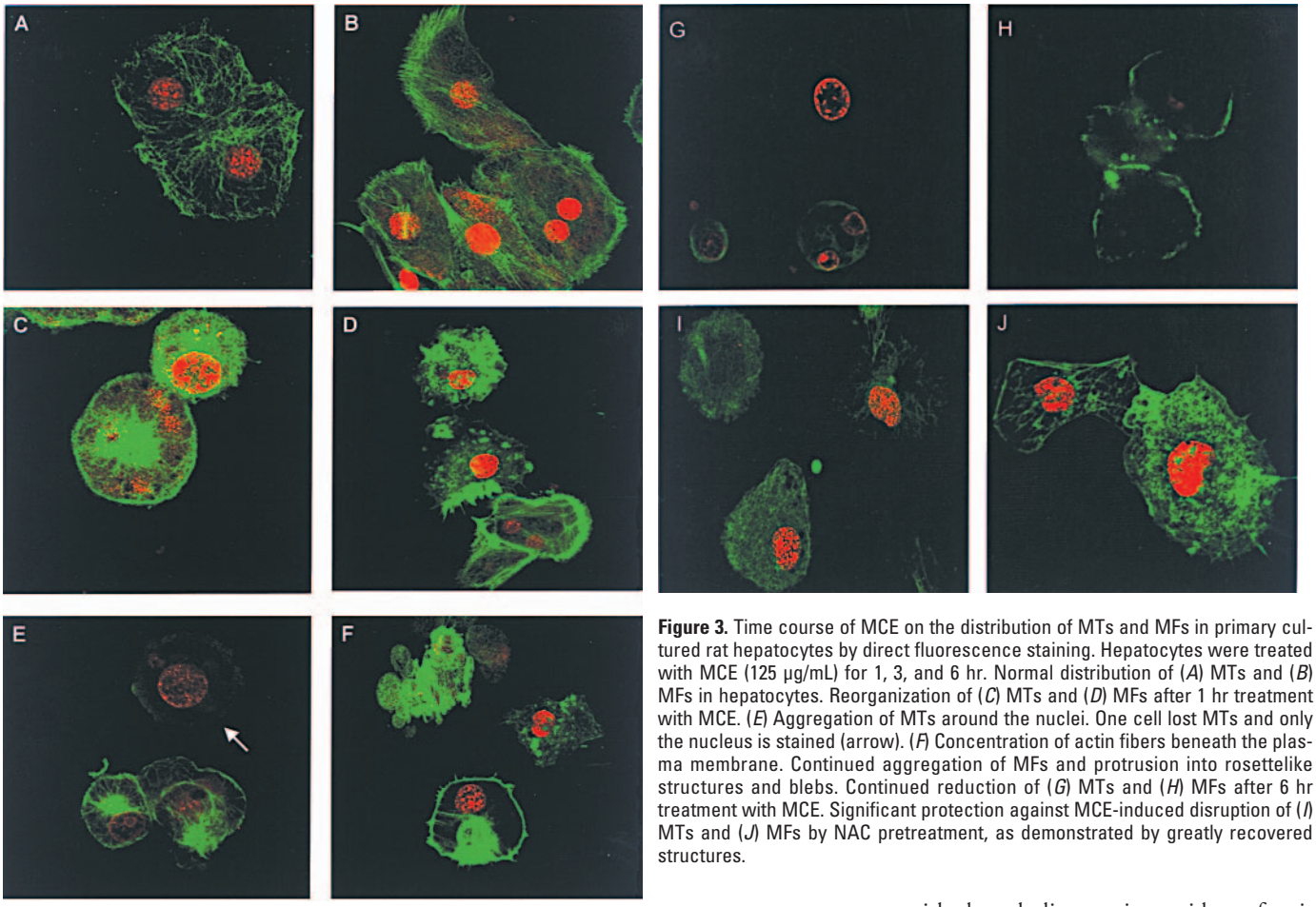


**Figure 3.** Time course of MCE on the distribution of MTs and MFs in primary cultured rat hepatocytes by direct fluorescence staining. Hepatocytes were treated with MCE (125 µg/mL) for 1, 3, and 6 hr. Normal distribution of (*A*) MTs and (*B*) MFs in hepatocytes. Reorganization of (*C*) MTs and (*D*) MFs after 1 hr treatment with MCE. (*E*) Aggregation of MTs around the nuclei. One cell lost MTs and only the nucleus is stained (arrow). (*F*) Concentration of actin fibers beneath the plasma membrane. Continued aggregation of MFs and protrusion into rosettelike structures and blebs. Continued reduction of (*G*) MTs and (*H*) MFs after 6 hr treatment with MCE. Significant protection against MCE-induced disruption of (*I*) MTs and (*J*) MFs by NAC pretreatment, as demonstrated by greatly recovered structures.

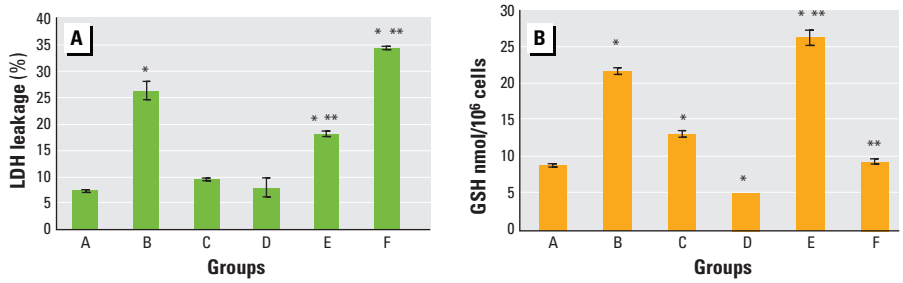


**Figure 4.** Effects of NAC and BSO pretreatment on the MCE-induced (*A*) LDH leakage and (*B*) GSH alterations in cultured rat hepatocytes. Data are means ± SD ($n = 3$) of three independent experiments. Group A, control; Group B, MCE (equivalent to 125 µg/mL lyophilized algae cells); Group C, NAC 10 mM; Group D, BSO 2.5 mM; Group E, MCE + NAC 10 mM pretreatment; Group F, MCE + BSO 2.5 mM pretreatment. Data were analyzed using Student's *t*-test.
*$p < 0.05$ as compared to control group. **$p < 0.05$ as compared to MCE.

structure (*32,33*). In our earlier study, we showed that MCE could induce ROS formation in rat hepatocytes with a relatively short exposure time (< 1 hr) (*27*). Therefore, MCE-induced ROS formation may play an important role in the disruption of MF structure, as observed in the present study.

In addition to the reorganization and aggregation of MTs induced by MCE in primary cultured rat hepatocytes, some cells lost MTs after MCE treatment. To our knowledge, this effect has not been previously reported in any cell type treated with microcystin. MTs are composed of α- and β-tubulin subunits, which contain 12 and 8 cysteine residues, respectively (*17*). Cellular GSH acts as a buffer to maintain protein sulfhydryls in reduced form (*34*). Tubulin cysteine–SH groups in the reduced form are essential for microtubules to maintain their polymerization state (*35*). Recent studies showed that microcystins could conjugate with GSH and cysteine in both cell-free systems and in rat liver (*23–25*). Therefore, it is possible that microcystin may disrupt the cytoskeletal structure by directly binding with the tubulin cysteine residues after it enters the cells. Environmental carcinogens such as cadmium and arsenite have a high affinity to GSH and also to affect the cytoskeletal organization by blocking certain tubulin–SH groups (*22*). Tubulin synthesis is controlled by a unique autoregulatory feedback in which the pool of free (depolymerized) tubulin monomers regulates the level of new tubulin synthesis by modulating the stability of tubulin mRNA (*36*). The initial reaction of MCE-induced depolymerization of MTs may increase the level of free tubulin and thus trigger the feedback inhibition of new tubulin synthesis. This would further impair the formation of intact microtubules and may in part explain the severe loss of MTs in MCE-treated cells even though the intracellular GSH level was significantly increased. However, the increased GSH level may favor the assembly of MTs and maintain its stability. This important role of GSH has been further demonstrated in our present study: NAC could significantly alleviate MCE-induced MT and MF changes.

GSH is the major cellular nonprotein thiol reductant and participates in numerous cellular processes such as intermediary metabolism and protection of cells against oxidative stress (*37*). In the present study,

exposure to MCE for 6 hr showed a dose-dependent increase of intracellular GSH. However, the time-course study surprisingly revealed a biphasic response, i.e., a steady increase of GSH after 3 hr treatment and attainment of the highest concentration at approximately 6 hr, followed by a decrease after 12 hr. This biphasic cellular GSH response is not unique. Similar alterations have been reported when cells were exposed to cadmium and arsenite (*21*). The depletion of intracellular GSH when cells were treated with MCE for 24 hr is probably due to the toxic effect of MCE as a result of cell membrane damage that leads to cell lysis and GSH efflux.

The disruption of hepatocyte cytoskeleton by MCE probably plays a crucial role in its hepatotoxicty. MTs and MFs change after 1 hr exposure to MCE, whereas significant LDH leakage only occurred after 3 hr treatment. The initial MCE–GSH binding may trigger the synthesis of GSH, probably by activating γ-glutamylcysteine synthetase, the rate-limiting enzyme for GSH biosynthesis (*37*). The finding that BSO, an inhibitor of γ-glutamylcysteine synthetase, diminishes the MCE-induced increase of cellular GSH suggests that new GSH is being synthesized to overcome the low level of intracellular GSH. The increase of intracellular GSH is probably a cellular response to protect from the toxic effect induced by MCE. This hypothesis is further supported by the evidence that when cells were pretreated with NAC, MCE-induced cytotoxicity as well as cytoskeleton changes were significantly reduced.

In conclusion, we showed that MCE disrupted the cellular cytoskeleton and affected the homeostasis of cellular thiols in hepatocytes. These two changes could be the main cytotoxic effect of MCE. The increase of intracellular GSH soon after MCE treatment may protect the hepatotoxicity induced by MCE. However, whether MCE also induces phosphorylation of MAPS and consequently destabilizes MTs and/or is a secondary effect to IF changes remains to be determined.

## References and Notes


1. Carmichael WW. The toxins of cyanobacteria. Sci Am 270:78–86 (1994).
2. Honkanen RE, Zwiller J, Moore RE, Daily SL, Khatra BS, Dukelow M, Boynton AL. Characterization of microcystin-LR, a potent inhibitor of type 1 and 2A protein phosphatase. J Biol Chem 265:19401–19404 (1990).
3. Ressom R, Soong FS, Fitzgerald J, Turczynowicz L, Elsaadi O, Roder D, Maynard T, Falconer IR. Health Effects of Toxic Cyanobacteria (Blue-Green Algae). Canberra, ACT, Australia:Australian Government Publishing Service, 1994.
4. Pouria S, de Andrade A, Barbosa J, Cavalcanti RL, Barreto VT, Ward CJ, Preiser W, Poon GK, Neild GH, Codd GA. Fatal microcystin intoxication in haemodialysis unit in Caruaru, Brazil. Lancet 352:21–26 (1998).
5. Jochimsen EM, Carmichael WW, An JS, Cardo DM, Cookson ST, Holmes CE, Antunes MB, de Melo Filho DA, Lyra TM, Barreto VS, et al. Liver failure and death after exposure to microcystins at a hemodialysis center in Brazil. N Engl J Med 338:873–878 (1998).
6. Yu SZ, Chen G. Blue-green algae toxins and liver cancer. Chin J Cancer Res 6:7–9 (1994).
7. Yu SZ. Primary prevention of hepatocellular carcinoma. J Gastroenterol Hepatol 10:674–682 (1995).
8. Ding WX, Shen HM, Zhu HG, Ong CN. Genotoxicity of microcystic cyanobacteria extract of a water source in China. Mutat Res 442:69–77 (1999).
9. Mirura GA, Robinson, NA, Geisbert TW, Bostian KA, White JD, Pace JG. Comparison of in vivo and in vitro effects of microcystin-LR in fasted rats. Toxicon 27:1229–1240 (1989).
10. Pace JG, Robinson NA, Miura GA, Matson CF, Geisbert TW, White JD. Toxicity and kinetics of [$^3$H]microcystin-LR in isolated perfused rat livers. Toxicol Appl Pharmacol 107:391–401 (1991).
11. Rao PV, Bhattacharya R, Pant SC, Bhaskar AS. Toxicity evaluation of in vitro cultures of freshwater cyanobacteria *Microcystis aeruginosa*. I: Hepatotoxic and histopathological effects in rats. Biomed Environ Sci 8:254–264 (1995).
12. Eriksson JE, Brautigan DL, Vallee R, Olmsted J, Fujiki H, Goldman RD. Cytoskeletal integrity in interphase cells requires protein phosphatase activity. Proc Natl Acad Sci USA 89:11093–11097 (1992).
13. Toivola DM, Goldman RD, Garrod DR, Eriksson JE. Protein phosphatases maintain the organization and structure interactions of hepatic keratin intermediate filaments. J Cell Sci 110:23–33 (1997).
14. Eriksson JE, Paatero GII, Meriluoto, JAO, Codd GA, Kass GEN, Nicotera P, Orrenius S. Rapid microfilament reorganization induced in isolated rat hepatocytes by microcystin-LR, a cyclic peptide toxin. Exp Cell Res 185:86–100 (1989).
15. Eriksson JE, Toivola D, Meriluoto JAO, Karaki H, Han Y-G, Hartshorne D. Hepatocytes deformation induced by cyanobacteria toxins reflects inhibition of protein phosphatases. Biochem Biophys Res Commun 173:1347–1353 (1990).
16. Wickstrom ML, Khan SA, Haschek WM, Wyman JF, Eriksson JE, Schaeffer AJ, Beasley VR. Alterations in microtubules, intermediate filaments, and microfilaments induced by microcystin-LR in cultured cells. Toxicol Pathol 23:326–337 (1995).
17. Alberts B, Bray D, Lewis J, Raff M, Roberts K, Watson JD, eds. The cytoskeleton. In: Molecular Biology of Cell. New York:Garland Press, 1983;549–688.
18. Kuriyama R, Sakai H. Role of tubulin-SH groups in polymerization to microtubules. J Biochem 76:651–654 (1974).
19. Leung M-F, Chou I-N. Relationship between 1-chloro-2,4-dinitrobenzene-induced cytoskeletal perturbation and cellular glutathione. Cell Biol Toxicol 5:51–66 (1989).
20. Kletsas D, Barbieri D, Stathakos D, Botti B, Bergamini S, Tomasi A, Monti D, Malorni W, Franceschi C. The highly reduced sugar 2-deoxy-D-ribose induces apoptosis in human fibroblasts by reduced glutathione depletion and cytoskeleton disruption. Biochem Biophys Res Commun 243:416–425 (1999).
21. Li W, Chou I-N. Effects of sodium arsenite on the cytoskeleton and cellular glutathione levels in cultured cells. Toxicol Appl Pharmacol 114:132–139 (1992).
22. Li W, Zhao Y, Chou I-N. Alterations of cytoskeletal protein sulfhydryls and cellular glutathione in cultured cells exposed to cadmium and nickel ions. Toxicology 77:65–79 (1993).
23. Kondo F, Ikai Y, Oka H, Okumura M, Ishikawa N, Harada K, Matsuura K, Murata H, Suzuki M. Formation, characterization, and toxicity of the glutathione and cysteine conjugates of toxic heptapeptide microcystins. Chem Res Toxicol 5:591–596 (1992).
24. Kondo F, Matsumoto H, Yamada S, Ishikawa N, Ito E, Nagata S, Ueno Y, Suzuki M, Harada K. Detection and identification of metabolites of microcystins formed in vivo in mouse and rat livers. Chem Res Toxicol 9:1355–1359 (1996).
25. Pflugmacher S, Wiegand C, Oberemm A, Beattie KA, Krause E, Codd GA, Steinberg CEW. Identification of an enzymatically formed glutathione conjugate of the cyanobacterial hepatotoxin microcystin-LR: the first step of detoxication. Biochem Biophys Acta 1425:527–533 (1999).
26. Ding WX, Shen HM, Shen Y, Zhu HG, Ong CN. Microcystic cyanobacteria causes mitochondrial membrane potential alteration and reactive oxygen species formation in primary cultured rat hepatocytes. Environ Health Perspect 106:409–413 (1998).
27. Ding WX, Shen HM, Zhu HG, Ong CN. Studies on oxidative damage induced by cyanobacteria extract in primary cultured rat hepatocytes. Environ Res 78:12–18 (1998).
28. Hissin PJ, Hiff RA. Fluorometric method for determination of oxidized and reduced glutathione in tissues. Anal Biochem 74:214–226 (1976).
29. Chou Y-H, Bischoff JR, Beach D, Goldman RD. Intermediate filament reorganization during mitosis is mediated by P34$^{cdc2}$ phosphorylation of vimentin. Cell 62:1063–1071 (1990).
30. Brugg B, Matus A. Phosphorylation determines the binding of microtubule-associated protein 2 (MAP2) to microtubules in living cells. J Cell Biol 114:735–743 (1991).
31. Rahilly MA, Fleming S. A tumor promoter induces alterations in vinculin and actin distribution in human renal epithelium. J Pathol 166:283–288 (1992).
32. Milzani A, Dalledonne I, Vailati G, Colombo R. Paraquat induces actin assembly in depolymerizing conditions. FASEB J 11:261–270 (1997).
33. van Gorp RM, Broers JL, Reutelingsperger CP, Bronnenberg NM, Hornstra G, van Dam-Mieras MC, Heemskerk JW. Peroxide-induced membrane blebbing in endothelial cells associated with glutathione oxidation but not apoptosis. Am J Physiol 277:C20–28 (1999).
34. Monte D, Ross D, Bellomo G, Eklow L, Orrenius L. Iterations in intracellular thiol homeostasis during the metabolism of menadione by isolated rat hepatocytes. Arch Biochem Biophys 235:334–342 (1984)
35. Mellon M, Rebhum LI. Studies on the accessible sulfhydryls of polymerizable tubulin. In: Cell Motility. New York:Cold Spring Harbor Laboratory, 1976;1146–1164.
36. Ben-Ze'ev A, Farmer SR, Penman S. Mechanisms of regulating tubulin synthesis in cultured mammalian cells. Cell 17:319–325 (1979).
37. Meister A. New aspects of glutathione biochemistry and transport: selective alteration of glutathione metabolism. Fed Proc 43:3031–3032 (1984).